AIAA JOURNAL
Vol. 32, No. 6, June 1994

Role of Mixing in the Chemical Oxygen-Iodine Laser Reactions

J. A. Miller*
Air Force Institute of Technology, Wright-Patterson Air Force Base, Ohio 45433
and
E. J. Jumper†
University of Notre Dame, Notre Dame, Indiana 46556

The thin shear-layer equations are solved for a two-dimensional parallel jet of molecular iodine I_2, in an electronically excited, singlet-delta oxygen freestream, $O_2(^1\Delta)$, in an effort to better understand the influence of mixing on the dissociation of I_2. Comparisons of one-dimensional premixed cases with corresponding two-dimensional jet-mixed cases of varying jet velocity ratios (and therefore mixing rates) indicate that, counter to common belief, imperfect mixing, which results in initial regions of high I_2 concentrations, can lead to faster dissociation. Although a single jet geometry is used in the study, examination of species concentration profiles gives some insight into the rationale for designing jet-mixing schemes, in terms of diffusion depths for ground state and excited species, and jet heights and spacing. Such insights may help to better understand flow systems in which reactions between excited O_2 and I_2 are of prime importance, as they are in the chemical oxygen-iodine laser.

I. Introduction

Background

THE chemical oxygen-iodine laser (COIL) was first demonstrated in 1977.[1] COIL is a chemically pumped laser which operates on an electronic transition of the iodine atom as opposed to other chemical lasers that operate on molecular vibrational or rotational transitions. When mixed with electronically excited oxygen, $O_2(^1\Delta)$, iodine molecules dissociate into iodine atoms which are then pumped rapidly into the $(^2P_{1/2})$ electronic state.

$$O_2(^1\Delta) + I(^2P_{3/2}) \rightarrow O_2(^3\Sigma) + I^*(^2P_{1/2}) \quad (1)$$

Note that $I(^2P_{1/2})$ will be denoted as I^*. Stimulated emission on the dominant hyperfine transition ($F = 3 \rightarrow F = 4$) of the $I(^2P_{1/2}) \rightarrow I(^2P_{3/2})$ magnetic-dipole transition produces photons at 1.315 μm.

Singlet-delta oxygen $[O_2(^1\Delta)]$, an energetic metastable molecule, can be produced in high number densities by the reaction of chlorine in a basic, hydrogen-peroxide solution.

$$H_2O_2 + 2KOH + Cl_2 \rightarrow 2KCl + 2H_2O + O_2(^1\Delta) \quad (2)$$

Transition of the $O_2(^1\Delta)$ molecule directly to the ground state is spin forbidden giving $O_2(^1\Delta)$ a long radiative lifetime (3600 s). The primary loss mechanism for $O_2(^1\Delta)$ is homogeneous pooling.

$$O_2(^1\Delta) + O_2(^1\Delta) \rightarrow O_2(^1\Sigma) + O_2(^3\Sigma) \quad (3)$$

The singlet-sigma state of oxygen is rapidly quenched in the presence of water.

$$O_2(^1\Sigma) + H_2O \rightarrow O_2(^3\Sigma) + H_2O \quad (4)$$

Once the energy is transferred to the iodine atom, the primary energy loss mechanisms become energy pooling of $O_2(^1\Delta)$ and I^*,

$$O_2(^1\Delta) + I^* \rightarrow O_2(^1\Sigma) + I \quad (5)$$

and quenching of excited iodine by water

$$I^* + H_2O \rightarrow I + H_2O \quad (6)$$

The first 1977 COIL laser produced 4 mW of output power[1]; by the end of 1989, the COIL device described in Ref. 2 demonstrated its design goal of 25 kW. Even with this progress, accurately predicting the performance of COIL devices has proven to be difficult. A recent review of the state of COIL modeling concluded that, although some uncertainties still exist in the applicable kinetic rate equations and corresponding rates, predicting the dissociation of molecular iodine I_2 in an excited oxygen stream $O_2(^1\Delta)$ is the largest source of error in modeling the performance of chemical oxygen-iodine lasers.[3] Modeling and experimental experience suggest that much of the difficulty in modeling these devices is derived, not

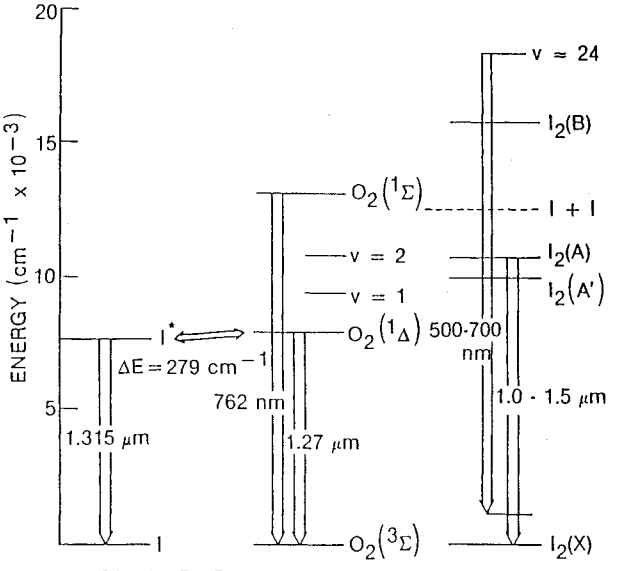

Fig. 1 O_2, I_2, and I energy level diagram.

Presented as Paper 90-0253 at the AIAA 28th Aerospace Sciences Meeting, Reno, NV, Jan. 8-11, 1990; received June 4, 1991; revision received Oct. 19, 1993; accepted for publication Jan. 16, 1994.

*Graduate Student, Department of Aeronautics and Astronautics.
†Associate Professor, Hessert Center for Aerospace Research, Department of Aerospace and Mechanical Engineering.

from a lack of understanding of the kinetics, but from errors in modeling the combined mixing and dissociation problem.[3-5]

Iodine Dissociation Chemistry

Originally, the dissociation of I_2 in an $O_2(^1\Delta)$ stream was attributed to a direct energy transfer from $O_2(^1\Sigma)$ (Refs. 6-8).

$$O_2(^1\Sigma) + I_2 \rightarrow O_2(^3\Sigma) + I + I \quad (7)$$

$O_2(^1\Sigma)$ is produced by the $O_2(^1\Delta)$ pooling reaction, Eq. (3). Referring to Fig. 1, which shows the relative energy levels of the species involved, the mechanism of Eq. (7) seemed plausible from an energy-level point of view; however, evidence from the first COIL lasing experiments showed that this mechanism was much too slow to account for the measured levels of dissociation. In particular, when high H_2O concentrations were introduced [which rapidly deplete $O_2(^1\Sigma)$ concentrations via Eq. (4)] little change in performance was observed.[9,10] This realization led to the discovery of an additional dissociation mechanism, a two-step process in which ground state I_2 is pumped to a highly excited vibrational level ($v \cong 43$) (denoted by $I_2^\dagger$) by a collision with either $O_2(^1\Delta)$, or with I^* (Refs. 11-14)

$$O_2(^1\Delta) + I_2 \rightarrow O_2(^3\Sigma) + I_2^\dagger \quad (8)$$

$$I^* + I_2 \rightarrow I + I_2^\dagger \quad (9)$$

A further collision of $I_2^\dagger$ with an $O_2(^1\Delta)$ leads to dissociation at near gas-kinetic rate.

$$O_2(^1\Delta) + I_2^\dagger \rightarrow O_2(^3\Sigma) + I + I \quad (10)$$

Pumping to the intermediate state by I^*, Eq. (9), is much faster than by $O_2(\Delta^1)$, Eq. (8) (see Table 1). Before the dissociation process begins no iodine atoms exist; consequently, the initial rate of dissociation is controlled, perhaps partially by the relatively slow energy transfer processes of Eq. (7), but more probably by the two-step process of Eqs. (8) and (10), especially in the presence of H_2O. As iodine atoms are formed, they are quickly pumped to the excited state via Eq. (1), and the rate of dissociation is accelerated by the reaction in Eq. (9). Thus, the rate controlling steps are handed off from Eqs. (8) and (10) [and, perhaps, Eq. (7)] to Eqs.(9) and (10), once sufficient I is available to be pumped via Eq. (1).

Purpose of this Study

The hand off of rate control, discussed in the previous subsection, could have an influence on laser design. Typically, because of the relatively short lifetime of I^*, I_2 is injected into the subsonic, excited oxygen stream just upstream of nozzles that accelerate the flow to supersonic as it enters the laser cavity.[2] If I_2 dissociations by direct impact with $O_2(^1\Sigma)$ and $O_2(^1\Delta)$ [Eqs. (7), (8), and (10)] are the only processes considered, the most efficient mixing scheme would be to rapidly mix the oxygen and iodine streams to achieve a uniform mixture.

Table 1 Reduced oxygen-iodine reaction set

	Kinetic process	Recommended rate coefficient, cm^3/molecule-s
1	$O_2(^1\Delta) + O_2(^1\Delta) \rightarrow O_2(^1\Sigma) + O_2(^3\Sigma)$	$k_1 = 2.7 \times 10^{-17}$
2	$O_2(^1\Sigma) + H_2O \rightarrow O_2(^3\Sigma) + H_2O$	$k_2 = 6.7 \times 10^{-12}$
3	$I_2 + O_2(^1\Sigma) \rightarrow I + I + O_2(^3\Sigma)$	$k_3 = 4.0 \times 10^{-12}$
4	$I_2 + O_2(^1\Delta) \rightarrow I_2^\dagger + O_2(^3\Sigma)$	$k_4 = 7.0 \times 10^{-15}$
5	$I_2 + I^* \rightarrow I_2^\dagger + I$	$k_5 = 3.8 \times 10^{-11}$
6	$I_2^\dagger + O_2(^1\Delta) \rightarrow I + I + O_2(^3\Sigma)$	$k_6 = 3.0 \times 10^{-10}$
7	$I_2^\dagger + H_2O \rightarrow I_2 + H_2O$	$k_7 = 3.0 \times 10^{-10}$
8	$I + O_2(^1\Delta) \rightarrow I^* + O_2(^3\Sigma)$	$k_8 = 7.8 \times 10^{-11}$
9	$I^* + O_2(^3\Sigma) \rightarrow I + O_2(^1\Delta)$	$k_9 = 2.7 \times 10^{-11}$
10	$I^* + O_2(^1\Delta) \rightarrow I + O_2(^1\Sigma)$	$k_{10} = 1.1 \times 10^{-13}$
11	$I^* + H_2O \rightarrow I + H_2O$	$k_{11} = 2.0 \times 10^{-12}$

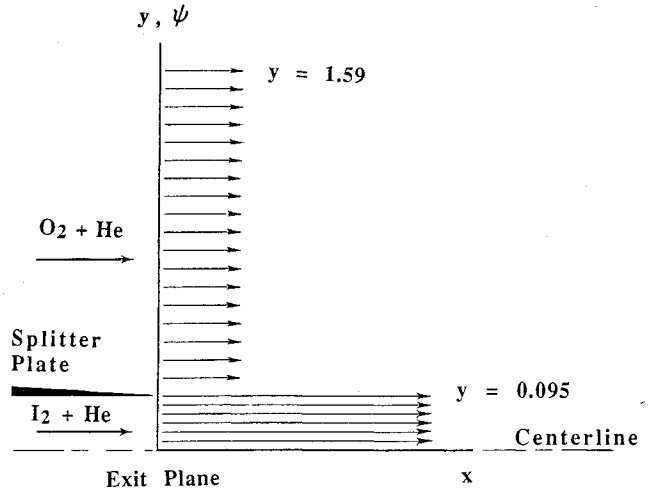

Fig. 2 Schematic of flow arrangement showing splitter plate and initial velocity profile for the freestream and jet for the 3/1 jet-mixed case.

Because of the acceleration of the dissociation process due to pumping of the intermediate, $I^\dagger$, by I^* [Eq. (9)], somewhat slower mixing schemes, resulting in regions of high I_2 concentrations, may result in faster and more complete dissociation; at the same time, the flows should be fully mixed once the iodine is fully dissociated. This being the case, the efficiency of a particular device depends heavily (perhaps entirely) on the mixing-scheme design.

The work reported on here is an attempt to begin to understand the fundamental role that mixing plays in the oxygen-iodine system. Because complex mixing geometries are both difficult to model and diagnose, the approach taken in this study was to investigate a simple mixing geometry. The mixing geometry selected was a two-dimensional, laminar, parallel jet with the pressure held constant, as shown schematically in Fig. 2. By varying the ratio of the jet velocity to the freestream velocity, the convection-enhanced mixing of an $O_2(^1\Delta)$ "freestream flow" into an I_2 "jet" can be adjusted. When the jet has a higher velocity than the freestream, the imposition of a constant pressure condition allows for the streamlines in the freestream to draw in toward the jet causing the $O_2(^1\Delta)$ to be drawn in toward the I_2 jet. Although the mixing geometry is simplified, the pressure, temperatures, and flow velocities used in this study are typical of the COIL device described in Ref. 2, in the subsonic mixing region of the device. The Reynolds number for the simple-geometry model ranged from approximately 30 to 200 based on the jet velocity and jet height. Although these low Reynolds numbers are not usually associated with turbulent flow, the potential for the inviscid Kelvin-Helmholtz-type shear-layer rollup at the edges of the jet exists[15]; however, the flow was not allowed to roll up. As such, the flow could be and was modeled using the thin shear-layer equations.

II. Modeling

Numerical Framework

The computational model selected for this study was a code described in detail elsewhere[16,17] and modified for the oxygen-iodine system (see details of modification in Refs. 5 and 18). The code numerically integrated the continuity, momentum, energy, and species equations in thin shear-layer (boundary-layer) form. The form of these equations was further simplified by transforming them from the two-dimensional (x-y) form to compressible stream function (x-ψ) form via the von Mises transformation.[18,19] This allowed for an explicit, forward-marching solution. Discussions of the numerical stability and maximum step size for this explicit formulation, in the presence of chemical-reaction complications, can be found in Refs. 5 and 18.

Thermodynamic and transport properties were computed at every numerical grid point based on the local temperature, pressure, and species. Polynomial fits of the enthalpy and specific heats for each species were used based on Ref. 20; mixture properties were formed as mass-fraction weighted sums. The viscosity of each species was calculated and formed into viscosity for the mixture following the real gas formulation in Ref. 21. The thermal conductivity for each species was computed using the Eucken approximation,[21] and the mixture conductivity was formed from that of the species in a manner similar to viscosity. The bimolecular diffusivity was computed for each species into each of the other species and then into the mixture following the approach given in Ref. 21. For more details see Refs. 5 and 16–18.

Chemical Reactions

It is known that more than 50 reactions play a role in a COIL device; however, sensitivity studies have shown that most of these reactions have little influence at standard COIL operating conditions.[3] These studies identified a reduced set of 11 reactions that essentially duplicate the results of the complete 50-reaction set.[3] Only these 11 reactions were used in our study; Table 1 lists these reactions along with their accepted empirical rate constants.

Note that each reaction is presented in terms of a forward rate constant. Where the rate for the reverse reaction is significant, it is listed as a separate reaction with a corresponding rate constant. For the system of excited oxygen and water vapor, the rate for reaction 1 has been measured along with the total removal of $O_2(^1\Delta)$ due to pooling $[O_2(^1\Delta) + O_2(^1\Delta)]$ to all other products. In this reduced set, the rate for reaction 2 has been selected to produce the same overall removal rate. A limited database does exist for the temperature dependence of some of these rates; these rates are presented in Table 2; these temperature dependences were incorporated into the computations. Details on the use of the Table 1 and Table 2 rates to compute the change in species in the computations can be found in Refs. 5 and 18.

Table 2 Available temperature dependent rate data (subscript numbers on *k* refer to numbers of reactions in Table 1)

$k_1 = 9.5 \times 10^{-28}\ T^{3.8}\ e^{(700/T)}$
$k_5 = 1.4 \times 10^{-19}\ e^{(1660/T)}$
$k_8 = 2.33 \times 10^{-8}/T$
$k_9 = (3.810^{-8}/T)\ e^{(-403/T)}$
$k_{10} = 4.0 \times 10^{-24}\ T^{3.8}\ e^{(700/T)}$

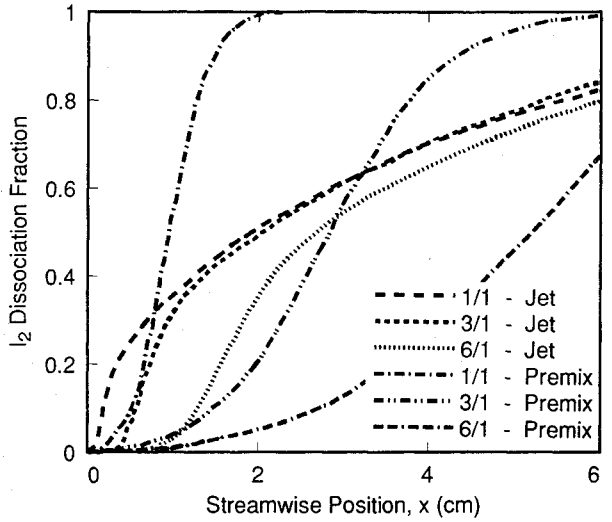

Fig. 3 Comparison of the streamwise variation in I_2 dissociation for the premixed and jet-mixed cases.

Boundary Conditions

Being an explicit formulation, only the initial conditions and streamwise pressure distribution were required. As mentioned earlier, the pressure was held constant. The initial geometry and velocities were specified as shown schematically in Fig. 2; the jet half-height was 0.095 cm and the outermost streamline for the freestream was at a half-height of 1.59 cm. The inlet velocity distribution was top-hat shaped as shown in Fig. 2. The centerline streamline was set at $y = 0.0$ and the corresponding stream function was set to zero and symmetry imposed there by requiring gradients in the stream function direction to be zero. This gradient condition was also imposed at the outermost stream function. The y location of the outermost stream function was set at the plane normal to the x direction at the edge (exit) of the splitter plate ($x = 0.0$) but was allowed to draw in (or out) as the computation progressed, as dictated primarily by the momentum transfer to the freestream flow from the jet. The initial species concentrations in the O_2 + He stream and the I_2 + He jet are discussed subsequently.

III. Results and Discussion of Mixing Studies

Table 3 lists the initial conditions for three jet-mixing cases with varying ratios of the jet (I_2 and diluent) velocity to the freestream (O_2 and diluent) velocity. At the lower limit, this ratio was set to 1 so that the mixing between the two streams was due solely to "unassisted" molecular diffusion (i.e., the concentration gradients are not strained by the streamlines being drawn toward the jet). For an increasing jet velocity relative to the freestream velocity, the oxygen stream increases its momentum near the jet through shear, and its streamlines draw in toward the iodine jet as dictated by continuity; thus, the mixing is enhanced by convective transport of the oxygen toward the higher velocity iodine jet. This transport tends to increase the concentration gradient for molecular diffusion, thus enhancing the rate of molecular mixing. Velocity ratios (jet velocity to freestream velocity) of 1/1 (i.e., no shear), 3/1, and 6/1 were considered. Three "premixed" cases representing ideal instantaneous mixing of the oxygen and iodine streams corresponding to the three jet cases were also run. The initial conditions for these cases are listed in Table 4.

Finally, H_2O was the only source of deactivation of $O_2(^1\Sigma)$, I*, and $I_2^\dagger$ considered in this study. Initially H_2O concentrations were set to zero to separate the effect of mixing alone on I_2 dissociation from the combined effect of mixing and deactivation losses on dissociation. H_2O levels typical of a COIL device [i.e., introduced in the production of $O_2(^1\Delta)$ via Eq. (2)] were then studied under similar flow conditions to see if the presence of water affected the fundamental roll of mixing in the reaction.

Water-Free Cases

Streamwise Comparisons

Figure 3 is a comparison of the streamwise variation of the total (i.e., integrated over the entire transverse plane of the flowfield) fraction of I_2 that has been dissociated for the six water-free cases described earlier (i.e., three jet cases and three premix cases). An I_2 dissociation fraction of 1 corresponds to complete I_2 dissociation. Note that initially the rate of dissociation for all premixed cases is slower than that for the corresponding jet-mixed cases, although the premixed dissociation fraction eventually overtakes the jet-mixed cases. The early dissociation advantage is present even when the jet and freestream velocities are the same (i.e., a jet-velocity ratio of 1/1); however, this advantage is amplified by increasing the jet-velocity ratio. This enhancement is not simply an artifact of presenting the results as a function of position, as opposed to "mixing time"; mixing-time comparisons can be found in Ref. 5, but can be inferred from Fig. 3 by realizing that in all cases the "premix" results would collapse onto a single curve if plotted vs time [i.e., t = distance (x) divided by velocity].

Table 3 Initial conditions for jet-mixing cases

Velocity ratio	1/1	3/1	6/1
Freestream			
T, K	300.0	300.0	300.0
P, dyn/cm^2	2.979×10^4	3.144×10^4	3.363×10^4
V, cm/s	6228.4	5900.8	5518.9
Mole fractions			
$O_2(^3\Sigma)$	0.15	0.15	0.15
$O_2(^1\Delta)$	0.10	0.10	0.10
$O_2(^1\Sigma)$	0.0	0.0	0.0
He	0.75	0.75	0.75
Jet			
T, K	400.0	400.0	400.0
P, dyn/cm^2	2.979×10^4	3.144×10^4	3.363×10^4
V, cm/s	6228.4	17702.5	31273.8
Mole fractions			
I_2	0.111	0.037	0.02
He	0.889	0.963	0.98

Table 4 Initial conditions for the one-dimensional, premixed cases

Associated jet case	1/1	3/1	6/1
T, K	400.0	400.0	400.0
P, dyn/cm^2	2.979×10^4	3.144×10^4	3.363×10^4
V, cm/s	6228.4	17702.5	31273.8
Mole fractions			
$O_2(^3\Sigma)$	0.1435	0.1322	0.1195
$O_2(^1\Delta)$	0.0957	0.0881	0.0797
$O_2(^1\Sigma)$	0.0	0.0	0.0
I_2	0.0048	0.0044	0.0040
He	0.7560	0.7753	0.7968

With this in mind, it can be seen from Fig. 3 that increased jet-velocity ratios increase the time over which the jet-mixed cases show an advantage over the premixed cases. Further, the global integration over the transverse plane to obtain the dissociation fraction for the jet-mixed cases masks the true advantage of mixing in accelerating the dissociation, since the jet height to freestream height was chosen for the purpose of a simplified study only. To explore the "local" advantage of mixing on I_2 dissociation, a more detailed view of the mixing is needed.

A somewhat more detailed picture of the role of the mixing is afforded by examining the change in species at the dividing streamline that originates at the splitter plate. The variation of the species concentrations at this "jet-boundary" streamline as a function of downstream position for the 6/1 jet-mixed case is shown in Fig. 4, with the corresponding premixed case shown in Fig. 5. A comparison of these figures shows a higher initial concentration of I_2 for the jet-mixed case with a corresponding rapid rise in the concentrations of I, I*, and, most importantly, $I_2^{\ddagger}$. The result is a much more rapid rate of dissociation for the jet-mixed case. The drop off in $I_2^{\ddagger}$ concentration near the 2-cm point occurs because the I_2 is being depleted by dissociation. The rate of formation of all of the excited species in the premixed case shows a more gradual rise; however, as is the case in the jet-mixed case, as the I* concentration builds the rate of dissociation increases due to a hand off between the slower dissociation mechanisms, Eqs. (7) or (8), and (10), and the faster mechanism of Eqs. (9) and (10). All of the jet-mixed cases display a rolloff in the dissociation rate as $O_2(^1\Delta)$ and I_2 are depleted at the jet interface, resulting in the eventual overtaking of the global dissociation fraction of Fig. 3 by the premixed cases for the geometry under study. The downstream location for this crossover in "dissociation success" for the global dissociation fraction of Fig. 3 is clearly a function of the jet-to-freestream velocity ratio, and, although not obvious, is geometry dependent (cf., what follows). Figures 4 and 5 show only the single dividing streamline at the jet-freestream interface. To gain a fuller understanding of why the rolloff occurs, it is instructive to take a more detailed look at the effect of mixing by examining transverse cuts through the flow at various streamwise locations.

Transverse Comparisons

Figures 6, 7, and 8 show the 6/1-jet-mixed, transverse profiles at streamwise locations of 1, 3, and 6 cm from the splitter plate exit plane, respectively, for the combined iodine mass fraction, $W(I + I_2)$, that includes both atomic and molecular iodine; the local I_2 dissociation fraction I_2 diss.; the total O_2 mass fraction $W(O_2)$; and the singlet-delta oxygen fraction $O_2(^1\Delta)/O_2$, commonly referred to as yield. The local I_2 dissociation fraction refers to the fraction of iodine atoms at a particular location to the total iodine (either I or I_2) at that location, so that a dissociation fraction of 1 corresponds to complete dissociation. Similarly, the $O_2(^1\Delta)$ fraction is the ratio of $O_2(^1\Delta)$ to total O_2 at a particular location. Laser "gain" is also shown in the figures; it is defined as

$$\text{gain} = \sigma([I^*]) - 0.5[I]) \tag{11}$$

where [ ] denotes atomic concentration (number/cm^3) and $\sigma = 5.7 \times 10^{-18}$ cm^2 is the stimulated emission cross section. Gain occurs where a population inversion has been achieved

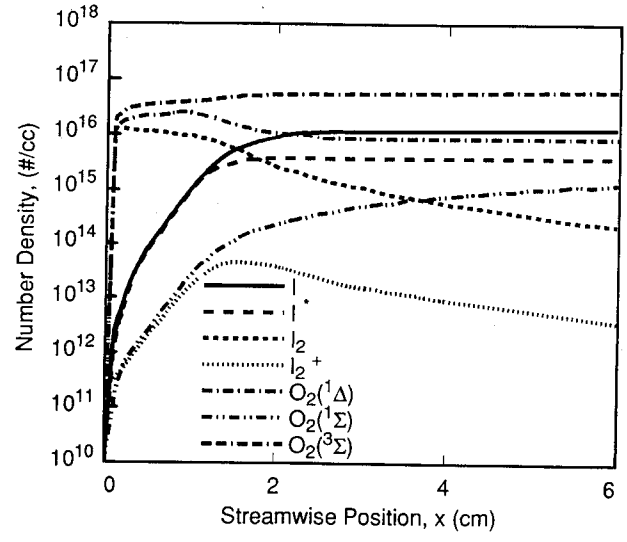

Fig. 4 Streamwise development of the species concentrations at the jet/freestream interface streamline just inside the I_2 jet, for the jet-mixed, 6/1 case.

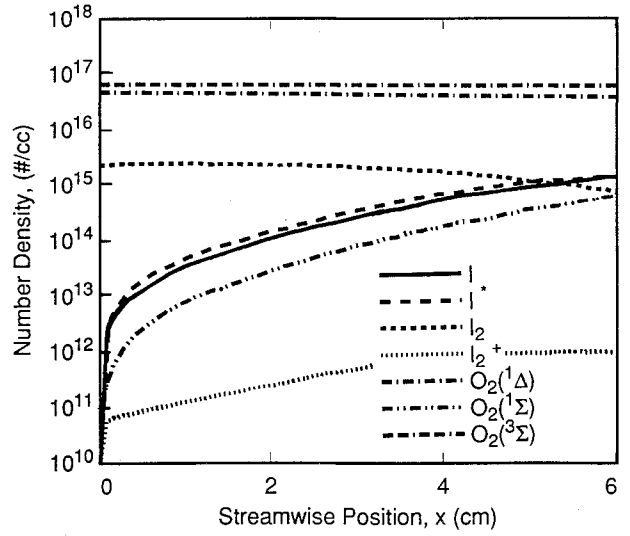

Fig. 5 Streamwise development of the species concentrations for the premixed, 6/1 case.

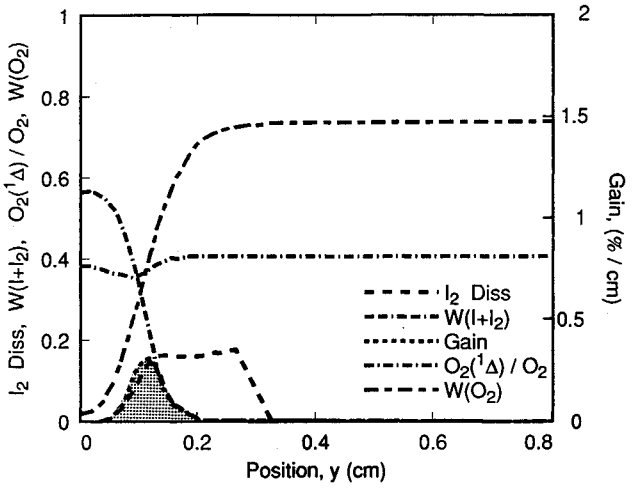

Fig. 6 Transverse profiles for total iodine mass fraction, oxygen mass fraction, iodine dissociation fraction, $O_2(^1\Delta)$ yield, and laser gain for the 6/1 jet-mixed case at $x = 1$ cm.

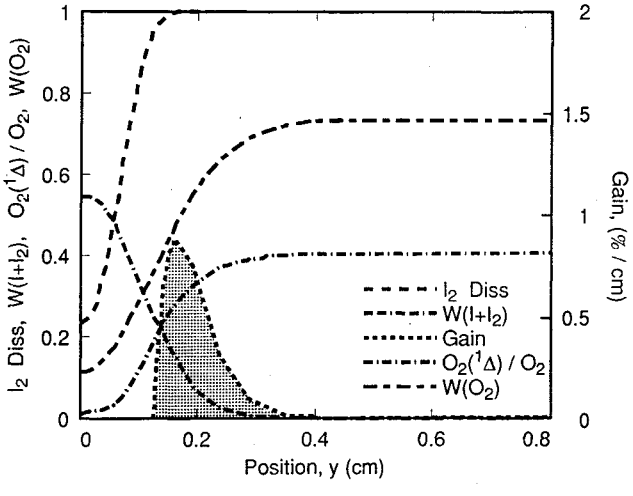

Fig. 7 Transverse profiles for total iodine mass fraction, oxygen mass fraction, iodine dissociation fraction, $O_2(^1\Delta)$ yield, and laser gain for the 6/1 jet-mixed case at $x = 3$ cm.

on atomic iodine indicating that lasing is possible. It can be shown that based on the equilibrium of the laser pump reaction, Eq. (1), a threshold $O_2(^1\Delta)$ fraction of 0.15 is required to produce gain at these conditions.

In Figs. 6–8, the origin for the y coordinate is the centerline (i.e., half the jet height at the splitter plate) and the initial boundary between the jet and freestream flows is at $y = 0.095$ cm; the profiles are displayed out to $y = 0.8$ cm, approximately half of the computational domain, since above $y = 0.8$ cm the freestream flow remains essentially undisturbed by the presence of the jet. Finally, it should be noted that the I_2 dissociation fraction is not plotted after the total iodine mass fraction falls below 0.001, since artificially high dissociation fractions (i.e., greater than 1) can occur in regions where the iodine concentrations are numerically very small.

Figure 6 shows that the O_2 and I_2 streams have only just begun to mix by the 1-cm location. The I_2 is only slightly dissociated in the mixing region (≈ 0.15). No dissociation has occurred in the core of the jet by this point. Note that gain can only occur where I_2 has dissociated to create I atoms and where the $O_2(^1\Delta)$ fraction is greater than the threshold value of 0.15. The gain profile in Fig. 6 illustrates this point.

As the flow progresses downstream (Figs. 7 and 8), the I_2 in the jet diffuses outward whereas the O_2 in the jet diffuses inward, aided by convective transport as the O_2 is drawn toward the faster-moving jet flow. Although the O_2 concentration on the jet centerline increases rapidly, the $O_2(^1\Delta)$ fraction actually drops to zero in the jet core. The I_2 which diffuses into the $O_2(^1\Delta)$-rich freestream is dissociated rapidly; however, the largest concentration of I_2 remains in the jet core even at $x = 6$ cm and nearly one half of the I_2 in the core remains undissociated. Note the location of the gain regions; contrary to what one might expect, the gain region moves outward toward the O_2 freestream as the jet expands, even though most of the I atom concentration is in the jet core. It now seems clear that the dropoff in the rate of dissociation in the streamwise direction for the jet-mixed cases in Fig. 3 occurs because the I_2 in the jet core becomes isolated from the $O_2(^1\Delta)$ in the freestream by a layer of completely dissociated iodine atoms. $O_2(^1\Delta)$ attempting to penetrate this layer is deactivated due to pumping of the I atoms via the reaction of Eq. (1), which accounts for the gain profile in this region. The dissociation rate becomes limited by the rate of transport of I_2 into the $O_2(^1\Delta)$ stream. These observations will be referred to again with regard to design considerations.

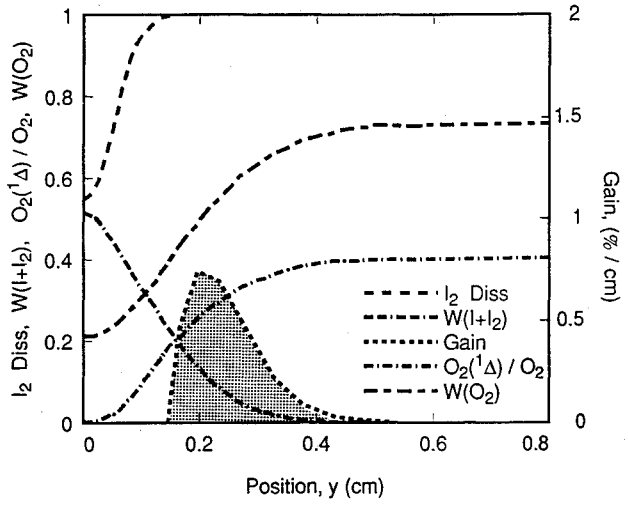

Fig. 8 Transverse profiles for total iodine mass fraction, oxygen mass fraction, iodine dissociation fraction, $O_2(^1\Delta)$ yield, and laser gain for the 6/1 jet-mixed case at $x = 6$ cm.

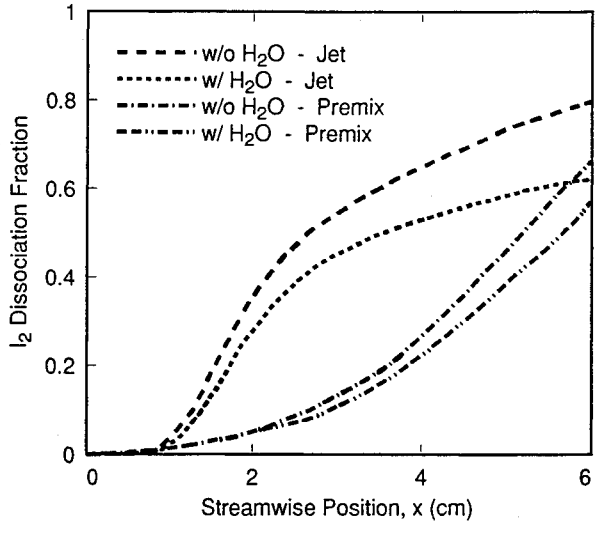

Fig. 9 Integrated streamwise effect of 2% (of O_2 flow) H_2O vapor on the I_2 dissociation for the 6/1 premixed and 6/1 jet-mixed cases.

Effect of Water Quenching

To investigate the role that H_2O has on the dissociation process, 2% H_2O vapor (molar percentage of the O_2) was added to the initial conditions for the jet-mixed and associated premixed cases. For the jet-mixed case, the H_2O vapor was added to the O_2 stream only, as physically realistic because H_2O vapor is introduced by the $O_2(^1\Delta)$ generator via Eq. (2). The integrated effect of H_2O on the I_2 dissociation fraction for both these cases is seen in Fig. 9. As expected, the H_2O interferes with the dissociation process [by quenching $O_2(^1\Sigma)$ and I*, the initiators, and $I_2^\dagger$, the intermediate] resulting in slower dissociation rates for both the premixed and jet-mixed cases. The H_2O appears to have a more detrimental effect in the jet-mixed case; however, this may be due to the higher concentration of H_2O in the freestream than is the case for the premix (i.e., H_2O is spread over a larger volume in the premixed case). Elimination of H_2O from the O_2 flow has always been recognized as important to COIL performance; however, this is usually attributed to the fast quenching rate for I*, the lasing species. Figure 9 shows that H_2O plays an important role in retarding the I_2 dissociation process as well. Beyond these observations, little change in the conclusions drawn from the water-free cases appears justified. Thus, the fundamental role of mixing in the dissociation process remains the same as that which can be gleaned from the water-free analysis.

IV. Conclusions

Although this is far from an exhaustive study of the role of mixing in two-path chemical processes, it points out that the roll is critical. Ideas expressed openly in the literature, for example, that instantaneous mixing (i.e., near-premixed conditions) are synonymous with maximum I_2 dissociation efficiency[4,12] can be misleading. As has been shown here, less well-mixed, higher-concentration iodine regions, concomitant with the imposition of mixing, lead to a more rapid handoff of the rate-controlling step from the slow $O_2(^1\Sigma)$ and $O_2(^1\Delta)$ mechanisms to the faster I* to $I_2^\dagger$ mechanism.

The critical role of properly designing the jet-mixing geometry is also made clear; once atomic iodine is present in sufficient quantity, energy from the oxygen is stripped as it penetrates the atomic-iodine region. Thus, although oxygen and molecular iodine continue to mix in the core of the jet the oxygen is in the triplet-sigma ground state and cannot participate in further dissociation or pumping processes. Knowledge of these critical diffusion depths for effective penetration of excited oxygen could directly contribute to sizing of the jet height. Additionally, mixing heights of the iodine jet into the oxygen stream could directly influence the design of the number of jets and their space that would lead to early and complete dissociation. Computations similar to those presented here, but over an expanded parameter range might prove of sufficient detail to construct a set of design guidelines. Pressure gradients in the streamwise direction could also be imposed, with essentially no additional numerical complexity, that could simulate the proximity to the entrance of a supersonic nozzle as well as tracking the reactions as the flow is accelerated to supersonic speeds to enter the lasing cavity. This could aid in placing the streamwise location of the jets but, more importantly, would give the proper temperature effects caused by the expansion. Additional studies that include lasing would also be of interest.

Acknowledgment

Work contained in this paper was completed in part as a Thesis in the Department of Aeronautics and Astronautics, Air Force Institute of Technology, but was carried out at the former Air Force Weapons Laboratory, now part of the Phillips Laboratory, Albuquerque, New Mexico.

References

[1]McDermott, W. E., Pchelkin, N. R., Benard, D. J., and Bousek, R. R., "An Electronic Transition Chemical Laser," *Applied Physics Letters,* Vol. 32, 1978, pp. 469, 470.

[2]Bloembergne, N., and Patel, C. K. N., "Report to the American Physical Society of the Study Group on Science and Technology of Directed Energy Weapons," *Reviews of Modern Physics,* Vol. 59, No. 3, Pt. II, 1987, pp. S:1–202.

[3]Perram, G. P., and Hager, G. D., "The Standard Chemical Oxygen-Iodine Laser Kinetics Package," Air Force Weapons Lab., AFWL-TR-88-50, Kirtland AFB, NM, Oct. 1988.

[4]Mikatarian, R. R., Jumper, E. J., and Woolhiser, C. C., "Fluid Dynamic Issues in Continuous-Wave, Short-Wavelength Chemical Lasers," AIAA Paper 88-2748, June 1988.

[5]Miller, J. A., and Jumper, E. J., "Numerical Simulation of the Dissociation of I_2 by $O_2(^1\Delta)$ in a Two-Dimensional Parallel Jet," AIAA Paper 90-0253, Jan. 1990.

[6]Arnold, S. J., Finlayson, N., and Ogryzlo, E. A., "Some Novel Energy-Pooling Processes Involving $O_2(^1\Delta g)^*$," *Journal of Chemistry and Physics,* Vol. 44, 1966, pp. 2529, 2530.

[7]Derwent, R. G., and Thrush, B. A., "Measurements on $O_2(^1\Delta g)$ and $O_2(^1\Sigma g)^+$ in Discharge Flow Systems," *Transactions of the Faraday Society,* Vol. 67, 1971, pp. 2036–2043.

[8]Derwent, R. G., and Thrush, B. A., "Excitation of Iodine by Singlet Molecular Oxygen," *Journal of the Chemical Society, Faraday Transactions,* Vol. 2, 1972, pp. 720–728.

[9]Benard, D. J., McDermott, W. E., Pchelkin, N. R., and Bouseck, R. R., "Efficient Operation of a 100-W Transverse-Flow Oxygen-Iodine Chemical Laser," *Applied Physics Letters,* Vol. 34, 1978, pp. 40, 41.

[10]Heidner, R. F., III, Gardner, C. E., El-Sayed, T. M., and Segal, G. I., "Dissociation of I_2 in $O_2(^1\Delta)$ – I Atom Transfer Laser," *Chemical Physics Letter,* Vol. 81, July, 1981, pp. 142–146.

[11]Avilés, R. G., Muller, D. F., and Houston, P. L., "Quenching of Laser-Excited $O_2(b^1\Sigma g^+)$ by CO_2, H_2O, and I_2," *Applied Physics Letters,* Vol. 37, Aug. 1980, pp. 358–360.

[12]Heidner, R. F., III, Gardner, C. E., Segal, G. I., and El-Sayed, T. M., "Chain Reaction Mechanism for I_2 Dissociation in the $O_2(^1\Delta)$ – I Atom Laser," *Journal of Physical Chemistry,* Vol. 87, No. 13, 1983, pp. 2349–2360.

[13]Hall, G. E., Maninell, W. J., and Houston, P. L., "Electronic-to-Vibrational Energy Transfer from $I^*(5^2P_{1/2})$ to $I_2(25<v<43)$," *Journal of Physical Chemistry,* Vol. 87, 1983, pp. 2153–2161.

[14]Van Benthem, M. H., and Davis, S. J., "Detection of Vibrationally Excited I_2 in the Iodine Dissociation Region of Chemical Oxygen-Iodine Lasers," *Journal of Physical Chemistry,* Vol. 90, No. 5, 1986, pp. 902–905.

[15]Birkhoff, G., and Zarantaonello, E. H., *Jets, Wakes, and Cavities,* Academic Press, New York, 1957.

[16]Jumper, E. J., Wilkins, R. G., and Preppernau, B. L., "Adaptation of a Wall-Catalytic Fluorine Recombination Model to Fluid-Dynamic Computations in an HF Laser Nozzle," AIAA Paper 85-1598, July 1985.

[17]Jumper, E. J., Wilkins, R. G., and Preppernau, B. L., "Wall-Catalytic Fluorine Recombination in an HF Laser Nozzle," *AIAA Journal,* Vol. 26, No. 1, 1988, pp. 57–64.

[18]Miller, J. A., "Numerical Simulation of the Dissociation of I_2 by $O_2(^1\Delta)$ in a Two Dimensional Parallel Jet," M.S. Thesis, Air Force Inst. of Technology, AFIT/GAE/AA/89M-3, Wright-Patterson AFB, OH, March 1989.

[19]Schlicting, H. H., *Boundary Layer Theory,* 7th ed., McGraw-Hill, New York, 1979.

[20]Anon., "JANAF Thermochemical Table," Dow Chemical Co., Midland, MI, 1963.

[21]Bird, R. B., Stewart, W. E., and Lightfoot, E. N., *Transport Phenomena,* Wiley, New York, 1960.